A new microporous anion metal-organic framework as a platform for highly selective adsorption and separation of organic dyes

Yuan-Chun He,[a] Jin Yang,*[a] Wei-Qiu Kan,[b] Hong-Mei Zhang,[a] Ying-Ying Liu[a] and Jian-Fang Ma*[a]

[a] *Key Lab of Polyoxometalate Science, Department of Chemistry, Northeast Normal University, Changchun 130024, People's Republic of China*

[b] *School of Chemistry and Chemical Engineering, Huaiyin Normal University, Huaian 223300, People's Republic of China*

* Correspondence authors

E-mail: yangj808@nenu.edu.cn (J. Yang)

E-mail: majf247@yahoo.com (J.-F. Ma)

Fax: +86-431-85098620 (J.-F. Ma)

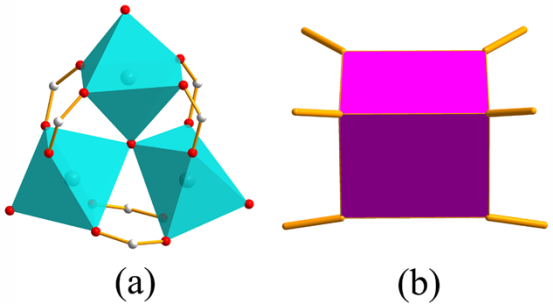

Fig. S1 View of the $Mn_3(\mu_3\text{-OH})$ cluster.

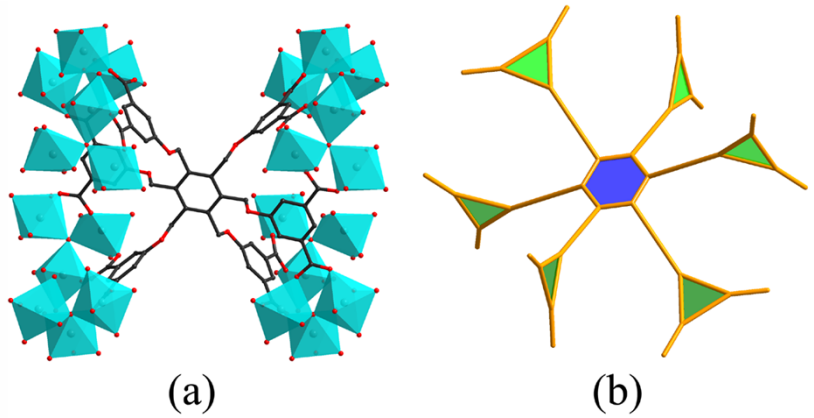

Fig. S2 Coordination mode of $H_{12}L$.

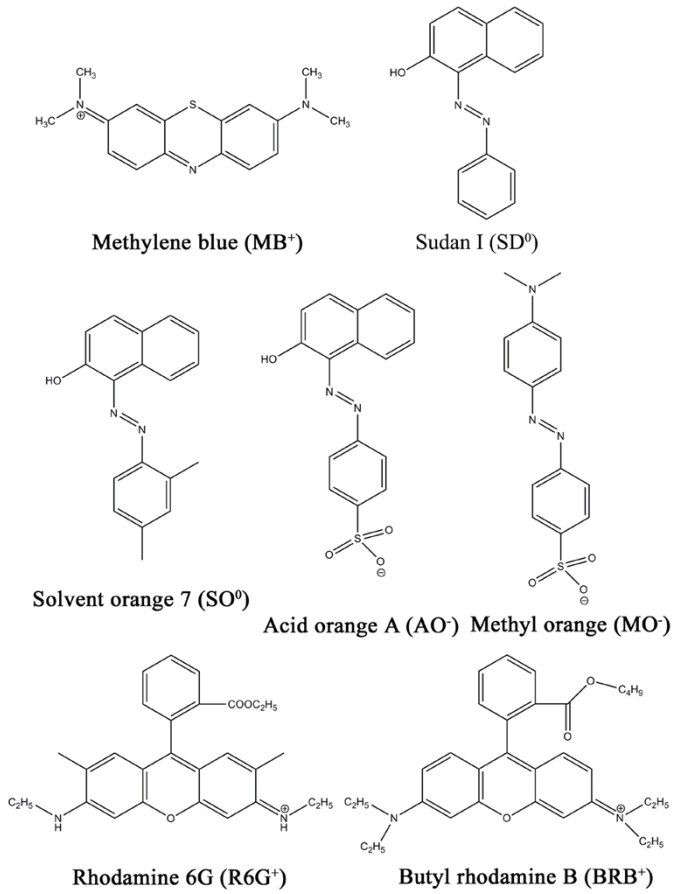

Fig. S3 Chemical structures of dyes used in this study.

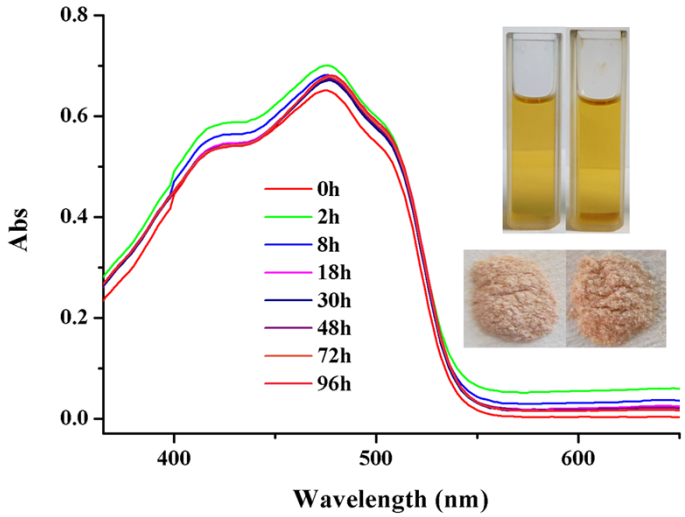

Fig. S4 Temporal evolution of UV-vis absorption spectra for **SD^0**.

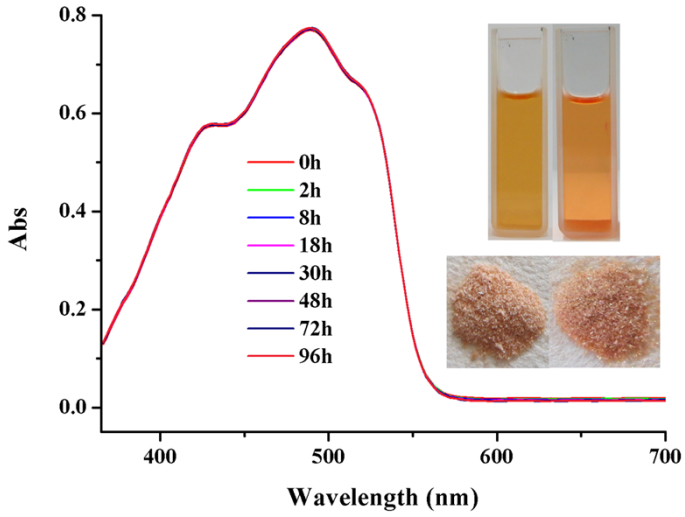

Fig. S5 Temporal evolution of UV-vis absorption spectra for **SO^0**.

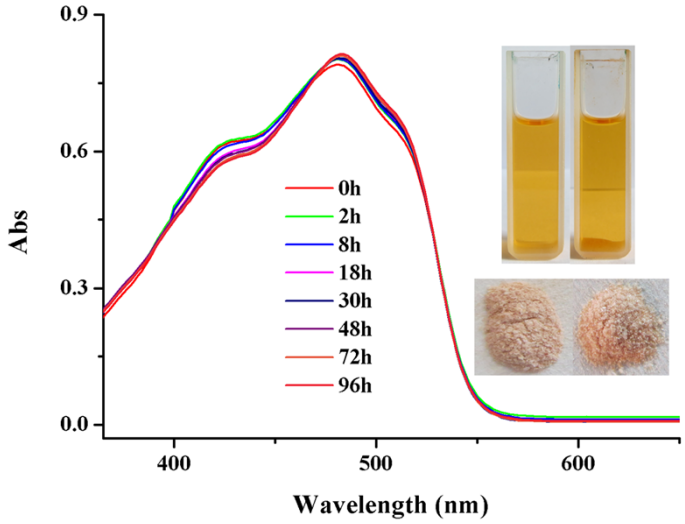

Fig. S6 Temporal evolution of UV-vis absorption spectra for **AO$^-$**.

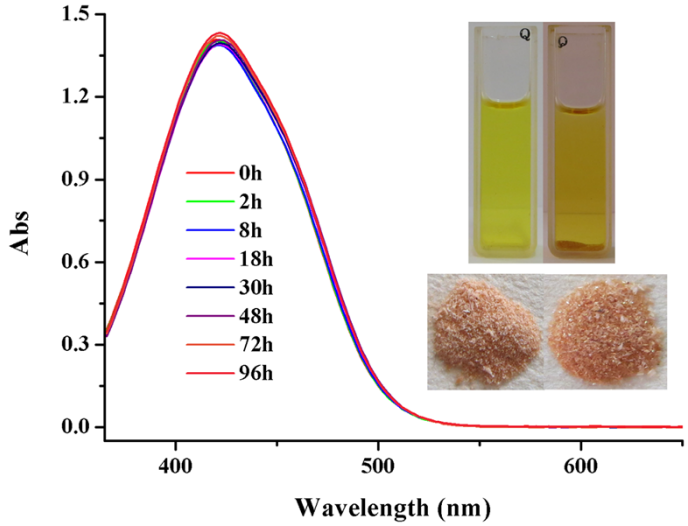

Fig. S7 Temporal evolution of UV-vis absorption spectra for **MO**$^{-}$.

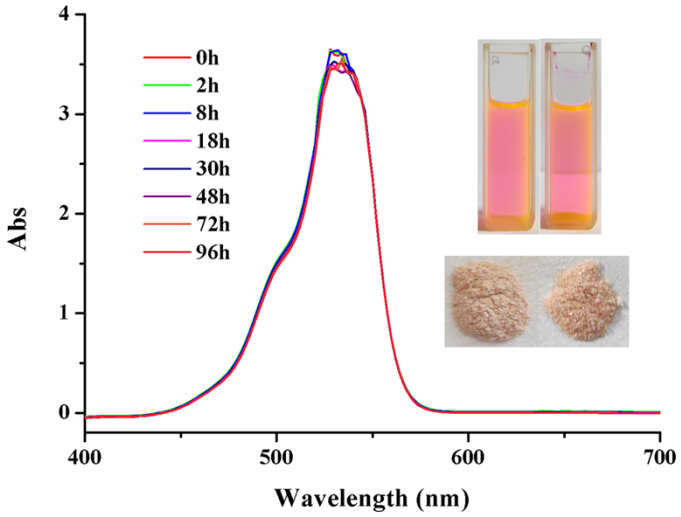

Fig. S8 Temporal evolution of UV-vis absorption spectra for **R6G**$^{+}$.

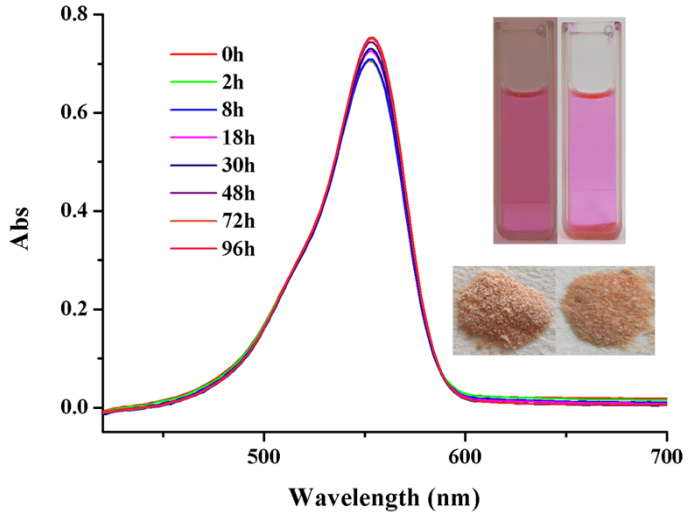

Fig. S9 Temporal evolution of UV-vis absorption spectra for **BRB**$^{+}$.

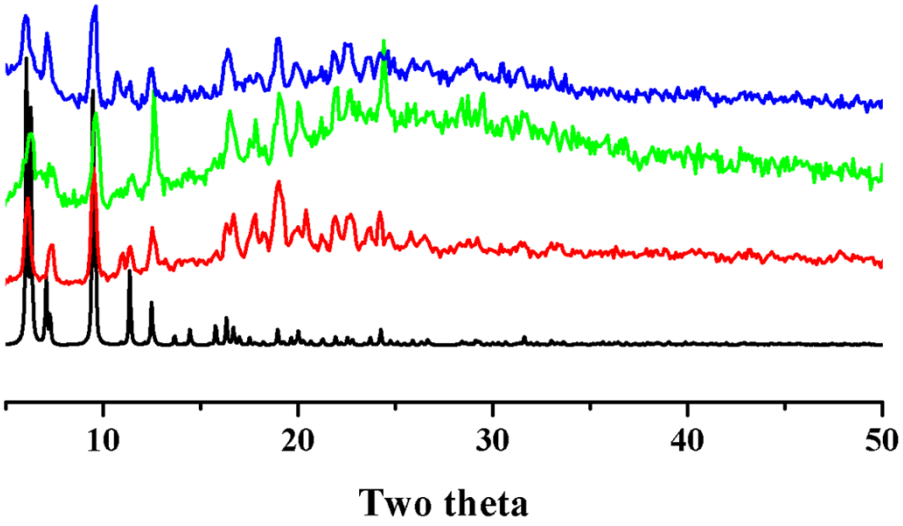

Fig. S10 PXRD patterns of **1** (black, simulated; red, as-synthesized; green, **MB**$^{+}$**@1**; blue, **MB**$^{+}$**@1** after **MB**$^{+}$ release).

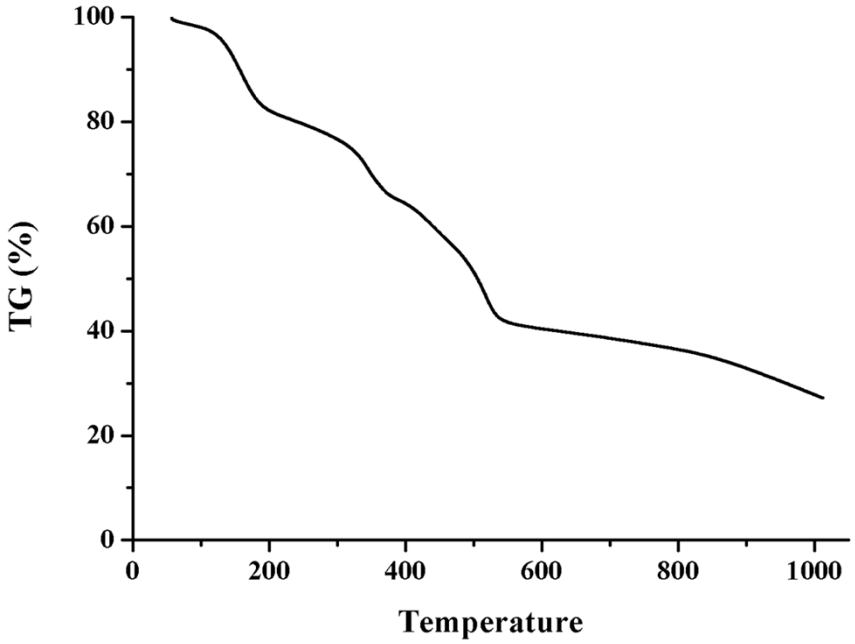

Fig. S11 TGA curve of **1**. The weight loss from room temperature to 198 °C is assigned to the removal of DEF molecules (obsd 17.7%, calcd 17.9%).

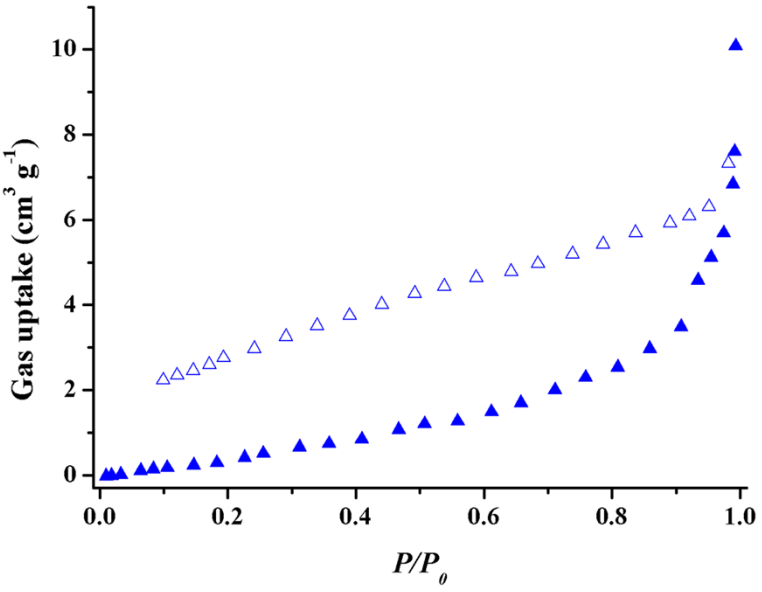

Fig. S12 N_2 adsorption isotherms at 77 K of the activated samples **1**. The activated samples were prepared by soaking the as-synthesized **1** in CH_3OH and then evacuation at 100 °C under vacuum. However, the N_2 uptake is very small. It is possible that the framework of **1** is collapsed after evacuation under vacuum.

Table S1 Crystal data and structure refinements for compound **1**.

	1
Formula	$C_{88}H_{112}Mn_6N_6O_{42}$
*M*r	2255.48
Space group	*P*-3*m*1
a/Å	28.1050(14)
b/Å	28.1050(14)
c/Å	14.5980(9)
V/Å^3	9986.0(9)
Z	3
D_c(g/cm^3)	1.125
GOF on F^2	1.123
*R*1 [I>2σ(I)]	0.0942

*wR*2 (all data)	0.2475
R_{int}	0.1248

Table S2 Selected bond distances (Å) and angles (°) for **1**.

Mn(1)-O(4)$^{\#1}$	2.136(4)	Mn(1)-O(9)	2.131(5)
Mn(1)-O(1)	2.140(4)	Mn(1)-O(1W)	2.183(7)
Mn(2)-O(2)	2.125(4)	Mn(2)-O(9)	2.127(5)
Mn(2)-O(2W)	2.188(7)	Mn(2)-O(8)$^{\#1}$	2.229(5)
Mn(3)-O(3W)	2.120(14)	Mn(3)-O(9)	2.094(5)
Mn(3)-O(7)$^{\#1}$	2.190(9)	Mn(3)-O(3)$^{\#1}$	2.170(6)
O(4)$^{\#1}$-Mn(1)-O(4)$^{\#2}$	95.6(2)	O(4)$^{\#1}$-Mn(1)-O(9)	91.93(15)
O(4)$^{\#1}$-Mn(1)-O(1)$^{\#3}$	86.08(17)	O(9)-Mn(1)-O(1)$^{\#3}$	90.14(16)
O(1)$^{\#3}$-Mn(1)-O(1)	92.1(3)	O(4)$^{\#1}$-Mn(1)-O(1W)	90.75(19)
O(9)-Mn(1)-O(1W)	176.0(2)	O(1)-Mn(1)-O(1W)	87.10(19)
O(2)-Mn(2)-O(2)$^{\#3}$	95.2(3)	O(2)-Mn(2)-O(9)	91.03(15)
O(2)-Mn(2)-O(2W)	88.6(2)	O(9)-Mn(2)-O(2W)	179.4(3)
O(2)-Mn(2)-O(8)$^{\#2}$	90.15(19)	O(9)-Mn(2)-O(8)$^{\#2}$	92.53(16)
O(2W)-Mn(2)-O(8)$^{\#2}$	87.9(2)	O(8)$^{\#2}$-Mn(2)-O(8)$^{\#1}$	84.3(3)
O(3W)-Mn(3)-O(9)	168.1(5)	O(3W)-Mn(3)-O(7)$^{\#1}$	101.8(4)
O(9)-Mn(3)-O(7)$^{\#1}$	71.3(3)	O(7)$^{\#1}$-Mn(3)-O(7)$^{\#2}$	102.9(5)
O(3W)-Mn(3)-O(3)$^{\#1}$	91.0(4)	O(7)$^{\#1}$-Mn(3)-O(3)$^{\#1}$	89.3(3)
O(9)-Mn(3)-O(3)$^{\#2}$	98.42(19)	O(3)$^{\#1}$-Mn(3)-O(3)$^{\#2}$	74.9(3)

Symmetry transformations used to generate equivalent atoms: $^{\#1}$ $-x+y$, y, $-z+2$; $^{\#2}$ x, y, $-z+2$; $^{\#3}$ x, $x-y$, z.